Magnetic properties of geometrically frustrated $Zn_xLi_{1-x}V_2O_4$

G.M. Kalvius[a], D.R. Noakes[b], R. Wäppling[c,*], N. Büttgen[d], A. Krimmel[d], M. Klemm[d], S. Horn[d], A. Loidl[d]

[a] *Physics Department, Technical University Munich, 85747 Garching, Germany*
[b] *Department of Physics, Virginia State University, Petersburg, VA 23806, USA*
[c] *Department of Physics, University of Uppsala, 75121 Uppsala, Sweden*
[d] *Institute for Physics, University of Augsburg, 86135 Augsburg, Germany*

Interest in $Zn_xLi_{1-x}V_2O_4$ is due to the fact that ZnV_2O_4 is an antiferromagnet, while LiV_2O_4 is the first example of a d-metal compound exhibiting heavy fermion behaviour [1–3]. The alloy series $Zn_xLi_{1-x}V_2O_4$ possesses the normal cubic spinel structure. Under the influence of nearest-neighbour antiferromagnetic exchange coupling, this structure exhibits geometric magnetic frustration. In ZnV_2O_4, however, a cubic to tetragonal structural phase transition at $T = 50\,K$ [4] removes, at least in part, the geometric frustration. This is not the case in the mixed compound $Zn_xLi_{1-x}V_2O_4$ and so behaviour related to stronger frustration is expected. The competition between heavy fermion behaviour and magnetism is pronounced [5]. An overview of bulk data and a discussion of aspects of frustration and heavy fermion properties can be found in Ref. [6]. The Augsburg group has recently published an evaluation of the ground-state properties of LiV_2O_4 and

*Corresponding author. Tel.: +46-18-471-3598; fax: +46-18-471-3524.
E-mail address: rogerw@fysik.uu.se (R. Wäppling).

$Zn_xLi_{1-x}(V_{1-y}Ti_y)_2O_4$ based on susceptibility, microwave resistivity, NMR and heat capacity measurements [7]. This work includes data on the $x = 0.2$ compound used in the present μSR study, thus allowing direct comparison between the findings from different techniques.

Part of our results from neutron diffraction, NMR and μSR for ZnV_2O_4 were published in a brief report [8]. The trigonal distortion occurring near 50 K, which was generally considered to relieve frustration, in fact only reduces it. The remaining frustration leads to the continuous development of a spin-glass-like magnetic precursor state, characterised by a fast exponential relaxation, between the paramagnetic state ($T > 38$ K) and the magnetic ground state ($T < 12$ K). The spectra can be described by the function:

$$A(t) = a_s \exp[-\lambda_e t] + a_f \exp[-\lambda_f t]. \quad (1)$$

It contains a slowly relaxing portion (a_s), whose rate connects directly to the paramagnetic rate and a fast relaxing portion (a_f), which is interpreted as the signature of a short-range correlated dynamic spin-glass-like state. The paramagnetic fraction a_s gets smaller on lowering the temperature and vanishes around 12 K, as shown in Fig. 1. Below 12 K, a Bessel-type oscillatory μSR response is

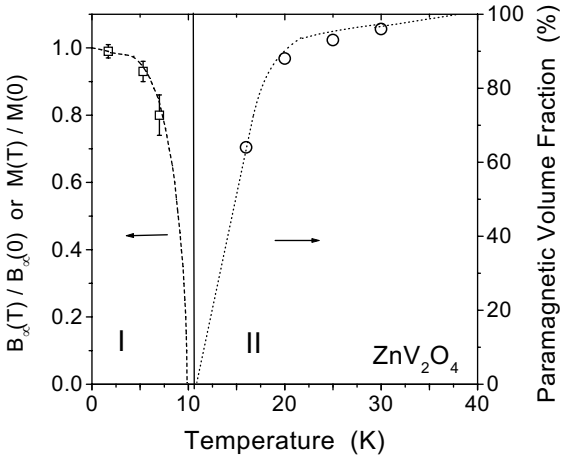

Fig. 1. The ZnV_2O_4 paramagnetic volume fraction (a_s of Eq. (1)) between 12 and 38 K (circles) and coherent oscillation field (B_μ of Eq. (2)) below 12 K, normalised to its low-temperature limit, $B_\mu(0) \sim 1.2$ kG (squares). The lines are guides for the eye.

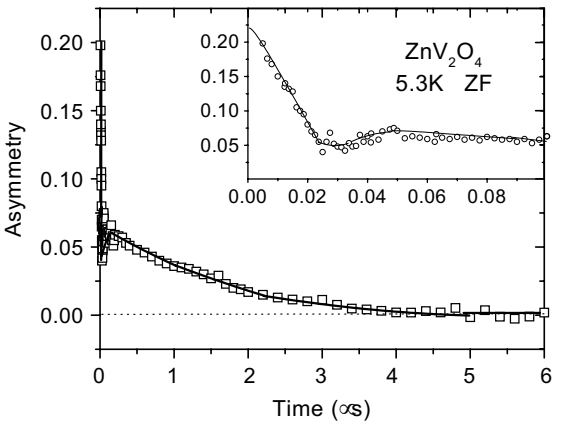

Fig. 2. ZF-μSR asymmetry spectrum of ZnV_2O_4 at 5.3 K (inset: early times with small time-bin size). The solid line is the least-squares fit of the incommensurate spin-density-wave model (Eq. (2)).

observed (see Fig. 2):

$$A(t) = a_0\{(2/3)J_0(\lambda_\mu B_\mu t)\exp[-\sigma_{trans}^2 t^2] + (1/3)\exp[-\lambda_{long} t]\}. \quad (2)$$

J_0 is the Bessel function of zero order, indicating an incommensurate spin density wave (ISDW) structure. a_0 is the signal strength, γ_μ the muon gyromagnetic ratio and B_μ the maximal field at the muon site (the latter is not known for this material). The temperature dependence of B_μ (shown in Fig. 1) is typical for a magnetic order parameter. The transverse relaxation rate σ_{trans} arises from random variations in the local field in addition to the distribution caused by the ISDW. This 'relaxing envelope' means that the ISDW structure has local disorder. The longitudinal relaxation rate λ_{long} reflects the dynamics of the spin assembly. The spectral parameters of ZnV_2O_4 and their meanings will be discussed further below.

Measurements on $Zn_{0.2}Li_{0.8}V_2O_4$ were performed on the M20 beam line at TRIUMF on a powder sample. We consider first the spectra above 12 K. In the analysis of those spectra one must realise that the spectral shape is sensitive to the application of small longitudinal fields B_{LF}. There are sizeable nuclear moments on ^{7}Li and ^{51}V (3.3 and 5.1 μ_n, respectively), but their action is complicated by electron–nuclear double

relaxation. Usually, ZF nuclear muon spin relaxation is described by a static Gaussian Kubo–Toyabe (sgkt) function $G^{\mathrm{sgkt}}(\Delta_{\mathrm{n}}, B_{\mathrm{LF}}, t)$, where Δ_{n} is the static width of the nuclear dipole field distribution at the muon site. In terms of the rms field at the muon site, $B_{\mathrm{rms}} = \gamma_{\mu}\Delta_{\mathrm{n}}$. In the present case, however, the nuclear relaxation might not be static since the electronic moments are located on vanadium, which also carries a nuclear moment, and hyperfine coupling may then lead to dynamic nuclear relaxation, especially in the vicinity of a magnetic transition. This situation has been discussed in detail for MnSi in Ref. [9] (see also Ref. [10]). Fig. 3 shows LF decoupling at 20 K. The data at 900 and 1800 G coincide with those at 300 G, meaning that the latter value is sufficient for maximal decoupling. The rms magnetic field for nuclear moments is typically of the order of a few Gauss corresponding to a static width Δ_{n} of about $0.5\,\mu\mathrm{s}^{-1}$. For a G^{sgkt} function, full decoupling is obtained at $B \sim 5\,B_{\mathrm{rms}}$. Only partial decoupling at 39 G in Fig. 3, to a relaxing (not horizontal) line, implies local-field dynamics. The solid lines in Fig. 3 are least-squares fits of the product of a dynamic Gaussian–Kubo–Toyabe (dgkt) function (nuclear relaxation) and an exponentially relaxing term (electronic relaxation):

$$A(t) = a_0 \exp[-\lambda_{\mathrm{e}} t] G^{\mathrm{dgkt}}(\Delta_{\mathrm{n}}, B_{\mathrm{LF}}, \tau_{\mathrm{n}}). \quad (3)$$

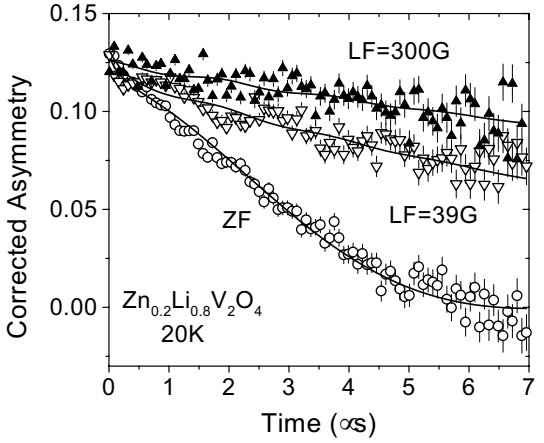

Fig. 3. ZF- and LF-μSR spectra of $Zn_{0.2}Li_{0.8}V_2O_4$ at 20 K. The spectra at 900 and 1800 G are indistinguishable from the spectrum at 300 G and were omitted for clarity. Solid lines are least-squares fits described in the text.

Satisfactory fits with a reasonable value for $\Delta_{\mathrm{n}} = 0.4\,\mu\mathrm{s}^{-1}$ and $1/\tau = 1\,\mathrm{MHz}$ (both practically independent of temperature) can now be obtained. The fact that this dynamic fit works at all temperatures down to as low as 15 K makes it unlikely that the effect is due to muon diffusion. The temperature dependence of the electronic relaxation rate λ_{e} is shown in Fig. 4: it changes from $0.51\,\mu\mathrm{s}^{-1}$ at 15 K to $0.05\,\mu\mathrm{s}^{-1}$ at 150 K. These are typical values for free paramagnetic spins.

There is a change in the ZF signal shape at 12 K. Fig. 5 demonstrates the presence of a rapidly decaying dynamic Gaussian–Kubo–Toyabe (dgkt) signal below this temperature. The later-time part of the ZF spectra of Fig. 5 and especially additional TF spectra at these temperatures reveal the presence of an additional slower-relaxing signal of exponential shape as well. The total fit function used for the ZF spectra in the low

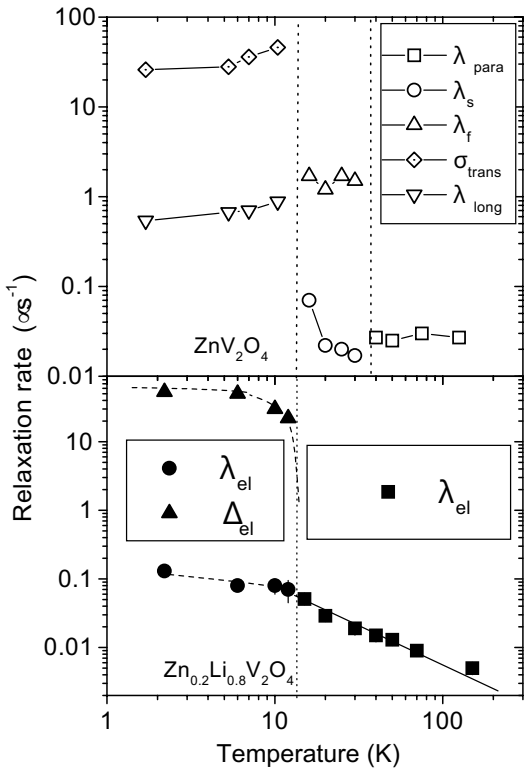

Fig. 4. Comparison of relaxation rates in ZnV_2O_4 and $Zn_{0.2}Li_{0.8}V_2O_4$. The lines are guides for the eye. For details, see text.

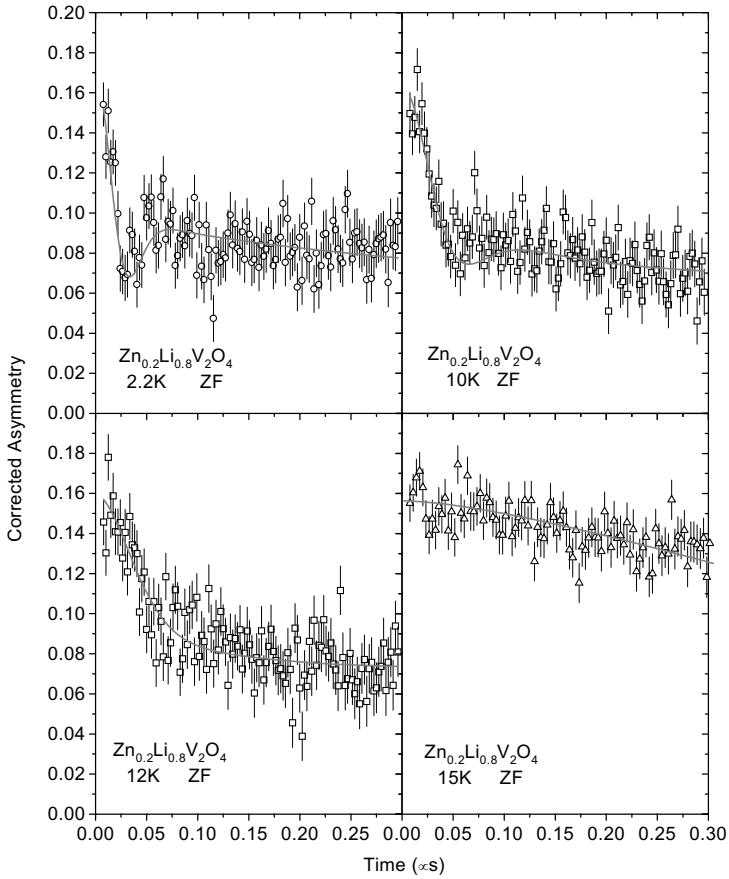

Fig. 5. Early portions of the ZF spectra of $Zn_{0.2}Li_{0.8}V_2O_4$ at 2.2, 10, 12 and 15 K. The solid lines are least-squares fits described in the text.

temperature range is

$$A(t) = a_f G^{dgkt}(\Delta_e, \tau, t) + a_s \exp[-\lambda_e t] G^{sgkt}(\Delta_n, t), \quad (4)$$

where the second term is the continuation of the paramagnetic signal, Eq. (3), but there is no longer enough information to distinguish the effect of a nuclear fluctuation rate $1/\tau_n$ from that of the electronic fields represented by λ_e, so the static nuclear Kubo–Toyabe function has been used. The dgkt function arises from a weakly dynamic random dense spin system. Δ_e reflects its static field distribution and $1/\tau$ is the fluctuation rate of the spins. This again is an inhomogeneous freezing model: a fraction a_s of the sample volume remains paramagnetic, while in the rest of the sample (fraction a_f) the electronic moments have entered a disordered, spin-glass-like state with slow magnetic dynamics. The effect of nuclear fields in relaxation in the frozen regions of the sample is completely negligible, and is ignored. G^{dgkt} is not affected by longitudinal fields up to ~ 2 kG. It can be seen in Fig. 5 that G^{dgkt} becomes increasingly dynamic on approaching the transition point at 12 K from below. The fluctuation rate $1/\tau$ varies smoothly from 25 MHz at 12 K to 5 MHz at 2 K. A static limit is not reached even at our lowest temperature. In summary, we have in the low temperature regime ($T < 12$ K) the coexistence of two spectral responses. Part of the muons sense a state similar to the paramagnetic state seen above 12 K, the other part senses a spin-glass-like, but not truly frozen, spin state. The intensity ratio of

the two signals a_f:a_s is about 2:1, the spin-glass-like state being more intense. This ratio does not change with temperature. The temperature dependence of the relaxation rates is shown in Fig. 4. The rate of the (paramagnetic) relaxation increases between 12 and 2.2 K from 0.75 to 1.5 μs^{-1}.

Fig. 4 also shows the temperature dependences of the relaxation rates for pure ZnV_2O_4, for comparison to $Zn_{0.2}Li_{0.8}V_2O_4$. In ZnV_2O_4 (Fig. 4, top), there are three regions. Above 38 K is the paramagnetic regime with a single low relaxation rate λ_{para} essentially independent of temperature. In particular, this rate shows no critical rise on approach to 38 K. Between 38 and 12 K, an inhomogeneous state is seen. It contains a persisting paramagnetic portion and short-range correlated dynamic spin-glass-like portion. The paramagnetic relaxation rate rises approaching 12 K, indicating that this is a magnetic transition point in contrast to the change at 38 K, which is the onset of spin freezing. Spin fluctuations in the spin-glass-like state are not dependent on temperature, i.e. they are solely determined by the spin–spin correlations. Below 12 K, one observes the signal of ordered magnetism, i.e. the sum of a transverse and a longitudinal signal as explicitly given in Eq. (2). The transverse relaxation rate σ_{trans} in Fig. 4 is large, meaning that considerable local spin disorder must exist. It is suggested that this excessive spin disorder is associated with a severe reduction in magnetic correlation length, that being the reason that neutron diffraction was unable to observe magnetic Bragg peaks [8]. It has been mentioned that the Bessel shape of the oscillatory signal (Fig. 1) suggests spin correlations of the incommensurate spin-density-wave type. The presence of dynamic short-range correlated spins above the magnetic ground state and a complex spin order with greatly reduced correlation length, coupled to the persistent spin fluctuations within the magnetic ground state, are signs of the presence of magnetic frustration in ZnV_2O_4. In contrast, the relaxation data for $Zn_{0.2}Li_{0.8}V_2O_4$ can be grouped into only two regions as seen in Fig. 4, bottom. Above 12 K one finds the paramagnetic state. Its relaxation rate as defined in Eq. (3) follows a critical law (i.e. a power law dependence) with an exponent around 1, suggesting that at 12 K a phase transition occurs. In Ref. [7], a critical behaviour on approach to 12 K is seen as well in NMR T_1 relaxation, in good agreement with the μSR data. The range of ZF-μSR paramagnetic relaxation rates is quite similar to that of ZnV_2O_4, if the paramagnetic signal of the mixed region between 38 and 12 K is included. Below 12 K in $Zn_{0.2}Li_{0.8}V_2O_4$, one finds the signal of a dense random spin system without long-range order. The spins are highly dynamic just below the transition point, then slow down appreciably but do not reach the static limit. In other words, no spin freezing occurs within the temperature interval investigated. The fact that neither freezing into a static spin glass state nor a transition into a long-range ordered state, even with moderate correlation length, takes place shows magnetic frustration to be stronger in $Zn_{0.2}Li_{0.8}V_2O_4$ than in ZnV_2O_4.

References

[1] S. Kondo, et al., Phys. Rev. Lett. 78 (2000) 372.
[2] O. Chmaissem, et al., Phys. Rev. Lett. 79 (1997) 4866.
[3] A. Krimmel, et al., Phys. Rev. Lett. 82 (1999) 2919.
[4] Y. Ueda, et al., J. Phys. Soc. Jpn. 66 (1997) 778.
[5] A. Krimmel, et al., Phys. Rev. B 61 (2000) 12578.
[6] S. Kondo, et al., J. Phys. Soc. Jpn. 69 (Suppl. B) (2000) 139.
[7] M. Brando, et al., Eur. Phys. J. B 22 (2002) 289.
[8] N. Büttgen, et al., Physica B 312–313 (2002) 703.
[9] R. Kadono, et al., Phys. Rev. B 42 (1990) 6515.
[10] D.R. Noakes, et al., Phys. Rev. B 35 (1987) 6597.